# Cell Death Inhibition Effect of Antioxidant Activity by 630 and 850 nm LEDs in RAW264.7 cells

Hee Eun Kim , Eun Young Kim , Jin-Chul Ahn [†] , SangJoon Mo [*,†]

Posted Date: 5 July 2023

doi: 10.20944/preprints202307.0212.v1

Keywords: oxidative stress; photobiomodulation; LED irradiation; cell death

*Article*

# Cell Death Inhibition Effect of Antioxidant Activity by 630 and 850 nm LEDs in RAW264.7 Cells

**Hee Eun Kim [1], Eun Young Kim [2], Jin Chul Ahn [2,3,†] and SangJoon Mo [3,4,5,†,*]**

[1] Department of Medicine, Graduate School of Medicine, Dankook University, Cheonan 31116, Republic of Korea
[2] Medical Laser Research Center, College of medicine, Dankook University, Cheonan 31116, Republic of Korea
[3] Photomedicine Research center, Dankook University, Cheonan 31116, Republic of Korea
[4] Center for Bio-Medical Engineering Core Facility, Dankook University, Cheonan 31116, Republic of Korea
[5] Department of Microbiology, Dankook University, Cheonan 31116, Republic of Korea
* Correspondence: sjmo1107@dankook.ac.kr; Tel:+82-41-550-1819
† These two authors contributed equally as co-corresponding authors.

**Abstract:** Phototherapy is an efficient strategy to respond to oxidative stress and has been in the spotlight in various therapeutic fields through its biological effect, but the exact molecular mechanism has not yet been established. As a result of irradiating RAW264.7 cells with a 630 nm or 850 nm LED with an energy intensity of 0.01J/cm$^2$, cell viability was increased depend on the irradiation time. After $H_2O_2$ was added, 630 nm or 850 nm LEDs were irradiated for 10 min or 40 min to increase cell viability by about 1.7- or 1.6-fold, respectively. In addition, 630nm or 850nm LED irradiation showed a significant ROS scavenging effect and significantly reduced TUNEL-positive cells by 45.7% and 37.8%, respectively, compared to cells treated only with $H_2O_2$. In the result of flow cytometry, the number of cells in the late apoptosis stage was about 2.3- and 1.8-fold lower than that of the cells treated with $H_2O_2$ only, but there was no significance. The Bax/Bcl-2 ratio of cells irradiated with 630 nm or 850 nm LED was significantly lower than that of cells treated with $H_2O_2$ only, and the expression of procaspase-3 and cleaved PARP was also significantly expressed in the direction of suppressing cell death. In conclusion, the ROS scavenging activity by 630 nm or 850 nm LED irradiation, leading the expression of cell death pathway proteins in the direction of inhibiting cell death.

**Keywords:** oxidative stress; photobiomodulation; LED irradiation; cell death

## 1. Introduction

Reactive oxygen species (ROS) such as dihydrogen dioxide ($H_2O_2$), superoxide anion radical ($O_2^-$), and hydroxyl radicals (OH•) are byproducts generated during oxygen consumption in the human body; all these ROS act as intracellular signaling molecules in vivo. ROS also play essential roles in the control of cellular functions such as the electron transport chain in mitochondria and the activation of white blood cells [1, 2]. However, excessive ROS cause oxidative stress by disrupting the antioxidant balance in the body. Free radical toxicity causes non-selective and irreversible damage to cellular components such as fat, protein, sugar, and DNA, leading to conditions such as cancer, Alzheimer's disease, heart disease, arteriosclerosis, inflammation, autoimmune diseases, and aging. A severe increase in the amount of ROS causes fatal damage to cells and eventually leads to cell death [3, 4].

Photobiomodulation (PBM) refers to irradiating light of a specific wavelength to induce and change spontaneous bioactivity in damaged areas of human tissue. Irradiated light has beneficial effects at power densities (irradiances) of 1 mW/cm$^2$ to 5 W/cm$^2$, with a narrow spectral width in the red or near-infrared region. PBM has been widely recognized in medical practice for > 50 years, and the recent use of PBM in an increasing range of pathologies has shown positive results [5, 6]. Several mechanisms have been proposed to explain the photobiological regulatory effects of PBM; the currently accepted hypothesis is that PBM of red/NIR light irradiated to cells or tissues is absorbed

 doi:10.20944/preprints202307.0212.v1



by mitochondria and promotes the production of adenosine triphosphate and nitric oxide; the generated adenosine triphosphate and nitric oxide promote the displacement of free radicals and the reduction of oxidative stress load on the organism by regulating the production of an appropriate amount of ROS when there is an imbalance between antioxidants and free radicals, activates transcription factors such as NF-κB that induce expression [7, 8]. PBM also enhances cell survival by upregulating the expression of protective proteins that prevent cell death [9–12]. Although the mechanism underlying PBM has not yet been fully elucidated, low-energy PBM yields more positive results compared with irradiation using light of the same wavelength at a higher energy. Notably, PBM can inhibit apoptosis and promote cell proliferation, migration, and adhesion under low-energy red or near-infrared light [13]. However, it remains unclear whether PBM can prevent intracellular oxidative stress-induced apoptosis. Because ROS have important roles in cell death, we hypothesized that PBM could inhibit cell death by protecting cells from ROS-induced damage.

The purposes of this study were to determine the protective effects of PBM on $H_2O_2$-induced cell death, then elucidate the mechanism underlying those effects. Our results suggest that PBM inhibits and protects against $H_2O_2$-mediated oxidative stress-induced cell death through the regulation of ROS generation and apoptosis.

## 2. Material and methods

### *2.1. Cell line and cell culture*

Mouse macrophage RAW264.7 cells were purchased from ATCC (Rockville, MD, USA), then cultured in Dulbecco's modified Eagle medium containing 10% (w/v) fetal bovine serum (35-015-CV; Corning, New York, NY, USA) and 1% (v/v) penicillin/streptomycin (30-002-CI; Corning, New York, NY, USA) at 37 °C with 5% $CO_2$; they were subcultured every 2 days.

### *2.2. Cell viability assay*

RAW264.7 cells were seeded in 96-well plates (30096; SPL Life Sciences Co., Ltd., Pocheon, Republic of Korea) at 5 × $10^3$ cells/well and cultured for 24 h, then treated with 0.6, 0.7, and 0.8 mM $H_2O_2$ for an additional 24 h. The cell culture medium was changed, 1 mg/mL of 3-[4,5-dimethylthiazol-2-yl]-2,5-diphenyltetrazolium bromide (MTT) was added, and cells were cultured for 3 h. After removal of the supernatant and addition of 150 μL dimethyl sulfoxide to melt the formed formazan crystals, the absorbance was evaluated at 570 nm using an ELISA reader (TECAN, Männedorf, Switzerland). Cell viability was indicated as a percentage of the untreated control group (i.e., not treated with $H_2O_2$).

### *2.3. LED irradiation and cytotoxicity*

LEDs of the same size (12.5 cm × 8.5 cm) with maximum emission wavelengths of 630 nm and 850 nm were used (Table 1). Cells were irradiated with either light source at a position approximately 5 cm from the bottom of the cell culture plate. Before irradiation, the power of the light source was measured as previously described [14, 15]. RAW264.7 cells (5 × $10^3$ cells/well) were seeded in 96-well plates and cultivated for 24 h at 37 °C with 5% $CO_2$. Then, 630 nm and 850 nm LEDs were respectively irradiated to the cells using an intensity of 10 mW/$cm^2$ at 5 min intervals for 20 min (total energy density: 3, 6, 9, and 12 J/$cm^2$). After irradiation, cells were cultured for 24 h and cell viability was measured as described above. To confirm that LED irradiation inhibited cytotoxicity in $H_2O_2$-treated cells, RAW264.7 cells were treated with 0.7 mM $H_2O_2$ and then irradiated with a 630 nm LED at 5-min intervals for 20 min (total energy density: 3, 6, 9, and 12 J/$cm^2$) and with an 850 nm LED at 10-min intervals for 40 min (total energy density: 6, 12, 18, and 24 J/$cm^2$). Cell viability was measured after 24 h as described above.

Preprints (www.preprints.org) | NOT PEER-REVIEWED | Posted: 5 July 2023 doi:10.20944/preprints202307.0212.v1



**Table 1.** LED information and parameters.

| **Manufacturer** | Wontech Co. Ltd., KOR | |
|---|---|---|
| **Light type** | Light emitting diode | |
| Number of array | 126 | |
| Mode | Continuous wave (CW) | |
| Wavelength (nm) | 630 (broadband: 600~650 nm) | 850 (broadband: 780~890 nm) |
| Aperture diameter (mm) | 2 | |
| Irradiance at aperture (mW/cm$^2$) | 10 | |
| Beam shape | Circular | |
| Beam profile | Gaussian | |

*2.4. ROS staining*

Cover slips were placed in 6-well plates (SPL Life Sciences Co., Ltd.) and RAW264.7 cells were grown at a density of 3 × 10$^5$ cells per well. After incubation for 24 h, 0.7 mM $H_2O_2$ was added; cells were then irradiated with a 630 nm or 850 nm LED, respectively, as described above. After incubation for 2 h, the culture medium was eliminated and cells were rinsed three times with 1 mL of 1 × phosphate-buffered saline (PBS) for 5 min. In dark conditions, 150 μL of 10 μM dichlorofluorescein diacetate (DCFDA) were added and cells were reacted for 15 min at room temperature; they were then washed three times (5 min per wash) with 1 mL of 1 × PBS. After removal of the cover slip and the surrounding PBS, VECTASHIELD solution containing 4,6-diamidino-2-phenylindole (DAPI; Vector Laboratories Inc., Burlingame, CA, USA) was added as a mounting medium. The stained samples were visualized using a fluorescence microscope by randomly setting three fields per cover slip (BX53F2, Olympus, Tokyo, Japan). ROS intensity was quantified using ImageJ software (NIH, Bethesda, MD, USA).

*2.5. TUNEL assay*

RAW264.7 (5 × 10$^5$ cells/well) cells were seeded on 6-well plates covered with cover slips, and cultured for 24 h. After incubation, each well was treated with 0.7 mM $H_2O_2$, then irradiated with a 630 nm or 850 nm LED at 10 mW/cm$^2$ for 10 min or 40 min, respectively. After incubation for 24 h, the culture medium was eliminated and the cells were rinsed twice with cold 1 × PBS, then fixed with 4% (v/v) paraformaldehyde (pH 7.4) dissolved in PBS at 4 °C for 25 min. Subsequently, cells were washed thrice for 5 min at 25 °C with 1 × PBS, permeabilized for 5 min at room temperature with 0.2% (w/v) Triton X-100 solution (9002-93-1; Sigma-Aldrich, Darmstadt, Germany) dissolved in PBS, and washed thrice for 5 min at room temperature with 1 × PBS. After remove cover slip and surrounding PBS, the cells were then covered with 100 μL of 1 × reaction buffer, incubated at room temperature for 5–10 min, and washed with 1 × PBS. Fifty microliters of staining solution prepared according to the manufacturer's instructions (5 μL of dUTP conjugated dye, 10 μL of 5 × reaction buffer, 1 μL of TdT recombinant enzyme, and 35 μL of deionized water; Bioacts, Incheon, Republic of Korea) were added to the cells, and then reacted in an incubator at 37 °C for 1 h. Cells were rinsed thrice with PBS at room temperature for 5 min to remove unreacted dye-dUTP. Next, they were incubated with propidium iodide (PI) solution (1 μg/mL) for 15 min at room temperature in the dark. After cells had been washed with PBS, VECTASHIELD mounting solution (Vector Laboratories Inc.) was added; a sample of three fields per cover slip was visualized with a confocal microscope, and cells showing a positive signal in each stain were counted and quantified (FV3000, Olympus, Tokyo, Japan).

*2.6. Flow cytometry analysis*

After RAW264.7 cells had been cultured for 24 h, treated with $H_2O_2$, and subjected to 630 nm or 850 nm LED irradiation, the medium was removed and cells were washed twice with 1 × cold PBS. Cells are detached by treatment with 0.25% Trypsin-EDTA (25200-056; Gibco, Waltham, MA, USA)

 doi:10.20944/preprints202307.0212.v1



and suspended in culture medium containing 10% FBS, then transferred to a new tube and centrifuged at 500 × g at 4 °C for 5 min to remove the supernatant. The cells were then rinsed with pre-chilled PBS and centrifuged at 500 × g for 5 min to remove the supernatant. Culture medium was added to resuspend the cells and the number of cells was determined. Next, cells were incubated at room temperature for 30 min and centrifuged again at 500 × g for 5 min, and the supernatant was removed. Then, cell apoptosis was measured by flow cytometry using the dead cell apoptosis kit (V13242; Thermo Fisher Scientific, Waltham, MA, USA) following manufacturer's instructions. In brief,1 × Annexin V binding solution (Thermo Fisher Scientific) was added to accomplish a final concentration of 1 × $10^6$ cells/mL, and 100 μL of the cell suspension was transferred to a new tube at a concentration of 1 × $10^5$ cells/100 μL. Then, 5 μL of fluorescein isothiocyanate (FITC) Annexin V (Thermo Fisher Scientific) and 1 μL of PI stock solution (100 μg/mL; Thermo Fisher Scientific) were added. Cells were incubated in the dark for 15 min at room temperature and then analyzed by flow cytometry by adding 100 μL of cold 1 × Annexin V solution (Thermo Fisher Scientific).

### *2.7. Western blotting analysis*

After adding $H_2O_2$, RAW264.7 cells irradiated with 630 nm or 850 nm LED were collected, respectively, and homogenized using ice-cold modified RIPA buffer [Biosesang, Seongnam, Republic of Korea; 50 mM Tris-HCl, 150 mM NaCl, 1 mM ethylenediaminetetraacetic acid, 1% (v/v) NP40, 1% (w/v) Triton X-100 (pH 7.4), and protease inhibitor cocktail]. Protein concentrations were determined using a protein assay kit (DC-protein assay kit, Bio-Rad, Hercules, CA, USA). Proteins were mixed with 5 × sample buffer (Bio-Rad). Proteins (40 μg per sample) were separated via 12% sodium dodecyl sulfate–polyacrylamide gel electrophoresis under reducing conditions, then transferred to polyvinylidene difluoride membranes (88520; Bio-Rad). Membranes were blocked with 5% (w/v) bovine serum albumin (BSA; to detect Bax, Bcl-2, and cleaved PARP proteins) or 5% (w/v) skim milk (to detect procaspase-3 protein) for 2 h. After they had been blocked, membranes were incubated with primary antibody (Bcl-2, 1:1000, Cell Signaling Technology, 3498s; Bax, 1:1000, Cell Signaling Technology, 14796s; procaspase-3, 1:1000, Cell Signaling Technology, 9662s; cleaved PARP, 1:200, Santa Cruz, sc-56196; *β*-actin, 1:1000, Sigma-Aldrich, A1978) in 5% BSA or 5% skim milk for 12 h at 4 °C. Membranes were washed four times with 0.1% (v/v) Tween-20 in PBS, then incubated with horseradish peroxidase-conjugated goat anti-rabbit or anti-mouse secondary antibody (LF8002; Ab Frontier, Seoul, Republic of Korea) for 1 h at room temperature. Ponceau staining was performed to monitor loading; bands were visualized using an enhanced electrogenerated chemiluminescence western blotting system (170-5061; Bio-Rad). Protein levels were analyzed and quantified using ImageJ (NIH).

### *2.8. Statistical analysis*

Independent experimental results are presented as mean ± standard deviation (SD). Comparisons of three groups or more than three groups of normally distributed data were accomplished by one-way ANOVA followed by multiple comparison tests to determine the least significant difference. Statistical analysis was employed GraphPad Prism software (ver. 7.0; San Diego, CA, USA). All experiments have been conducted in triplets and recognized as statistically significant differences when the *p*-value was less than 0.05.

## 3. Results

### *3.1. Cell viability after $H_2O_2$ treatment*

To confirm the viability of RAW264.7 cells after treatment with different concentrations of $H_2O_2$, cells were incubated with 0.6, 0.7, and 0.8 mM $H_2O_2$ for 24 h, then analyzed using MTT assays. As shown in Figure 1A, the number of cells decreased as the concentration of $H_2O_2$ increased; compared with the cell viability of untreated cells, the cell viabilities after treatment with 0.6, 0.7, and 0.8 mM $H_2O_2$ were 76.7%, 65.6%, and 26.4%, respectively (Figure 1B; $p < 0.05$, $p < 0.01$, and $p < 0.0001$,

Preprints (www.preprints.org) | NOT PEER-REVIEWED | Posted: 5 July 2023 doi:10.20944/preprints202307.0212.v1



respectively). Therefore, 0.7 mM $H_2O_2$ with a cell viability of 65% was used for subsequent experiments.

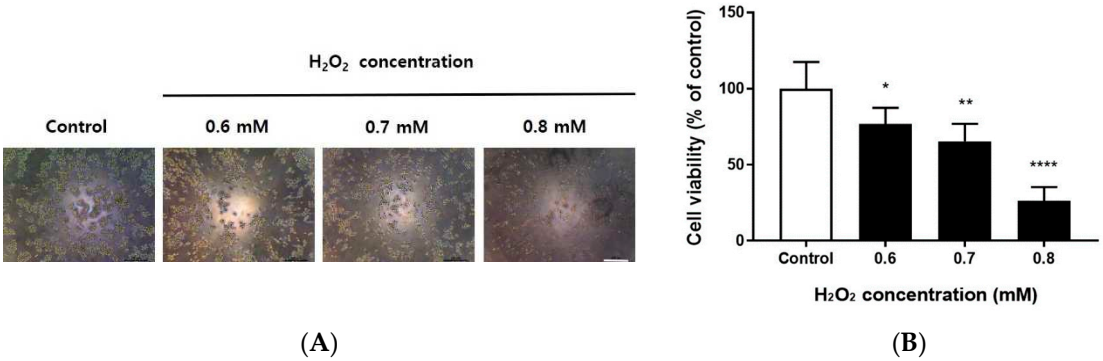


(**A**) (**B**)

**Figure 1.** Cell viability of $H_2O_2$-treated RAW264.7 cells. RAW264.7 cells were grown in 96-well culture plates ($1 \times 10^5$ cells/well) for 24 h, then treated with 0.6, 0.7, or 0.8 mM $H_2O_2$ for 24 h. (A) Cell morphology after treatment of RAW264.7 cells with 0.6, 0.7, or 0.8 mM $H_2O_2$ for 24 h. Cells were observed using an inverted microscope (magnification, 100×). Scale bar, 200 $\mu$m. (B) After 24 h, cell viability was determined by MTT assay. The percentage of cell viability was normalized to the untreated cells. Data are shown as means ± SD of values from three separate experiments (n = 3). ****$p < 0.0001$, **$p < 0.01$, and *$p < 0.05$ vs. untreated cells. One-way ANOVA and Sidak's post hoc analyses were performed to compare all experimental conditions.

*3.2. Cell viability after LED irradiation*

To assess the effects of 630 nm or 850 nm LED irradiation on cell viability, cells were irradiated with an intensity of 10 mW/cm² at 5 min intervals for up to 20 min (total energy density: 3, 6, 9, and 12 J/cm²). After cultured RAW264.7 cells had been irradiated with each of the LEDs for different lengths of time, the cells were cultured for a day and viability was measured. At 630 nm, cell viability tended to increase as the duration of LED irradiation increased. Notably, when irradiated with an intensity of 10 mW/cm² for 15 min (9 J/cm²) and 20 min (12 J/cm²), cell viability significantly increased by 106% and 109%, respectively, compared with the viability of non-irradiated cells (Figure 2A; $p < 0.05$ and $p < 0.001$, respectively). Furthermore, when irradiated with an intensity of 10 mW/cm² for 20 min (12 J/cm²) at 850 nm, cell viability significantly increased by 110% compared with non-irradiated cells (Figure 2B; $p < 0.05$). Thus, 630 nm or 850 nm LED irradiation did not affect RAW264.7 cell viability.

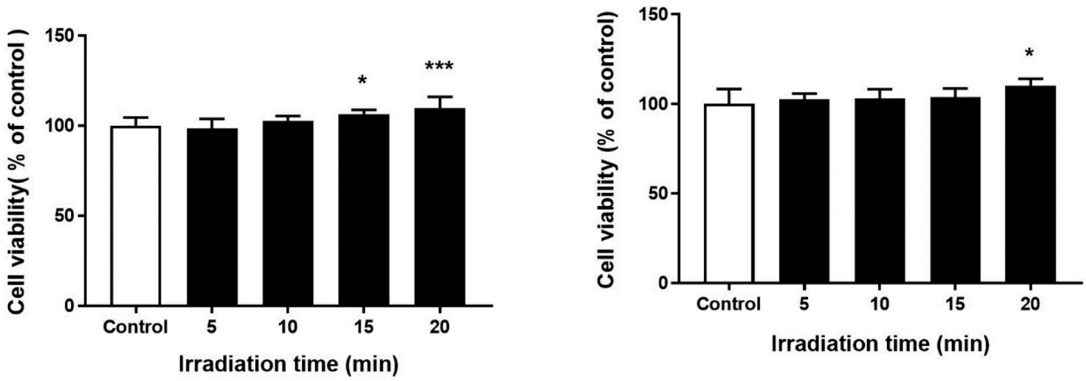


(**A**) (**B**)

**Figure 2.** Effect of 630 nm and 850 nm LEDs on the cell viability of RAW264.7 cells. RAW264.7 cells were irradiated using a 630 nm LED (A) or 850 nm LED (B) with an intensity of 10 mW/cm² at 5 min intervals for up to 20 min (total energy density: 3, 6, 9, and 12 J/cm²), then cultured for 48 h. Cell

Preprints (www.preprints.org) | NOT PEER-REVIEWED | Posted: 5 July 2023 doi:10.20944/preprints202307.0212.v1



viability was measured using colorimetric MTT metabolic activity assays. Each experiment was performed ≥ 3 times (n = 3). Data are shown as means ± SDs. *$p < 0.05$ and ***$p < 0.001$ vs. untreated cells. One-way ANOVA and Dunnett's post hoc analyses were performed to compare all experimental conditions.

### *3.3. Antioxidant effects of 630 nm and 850 nm LEDs*

To investigate the antioxidant effects of 630 nm or 850 nm LED irradiation, $H_2O_2$-treated RAW264.7 cells were subjected to each LED irradiation, followed by assessment of cell viability. After treatment with 0.7 mM $H_2O_2$, cells were irradiated by an LED with an intensity of 10 mW/cm$^2$. The 630 nm LED irradiation was performed at 5 min intervals for 20 min (total energy density: 3, 6, 9, and 12 J/cm$^2$); the 850 nm LED irradiation was performed at 10 min intervals for 40 min (total energy density: 6, 12, 18, and 24 J/cm$^2$). As shown in the results of Figure 3, the cell viability of RAW264.7 cells irradiated with 630 nm LEDs for 10 min (6 J/cm$^2$); after $H_2O_2$ treatment was significantly increased by about 1.7-fold compared to non-irradiated cells ($p < 0.001$), but showed a tendency to decrease after irradiation for 15 min (9 J/cm$^2$) and 20 min (12 J/cm$^2$) (Figure 3A). In contrast, cell viability gradually increased as the duration of 850 nm LED irradiation increased (Figure 3B). In particular, cell viability was significantly increased by approximately 1.6-fold after 40 minutes (24 J/cm$^2$) of irradiation, compared with the viability of non-irradiated cells ($p < 0.0001$). These results show the antioxidant effect of 630 nm and 850 nm LEDs on $H_2O_2$-induced oxidative stress. Therefore, subsequent experiments were performed using 10 and 40 min (6 and 24 J/cm$^2$, respectively) durations of irradiation with the 630 nm and 850 nm LEDs, respectively, at an intensity of 10 mW/cm$^2$.

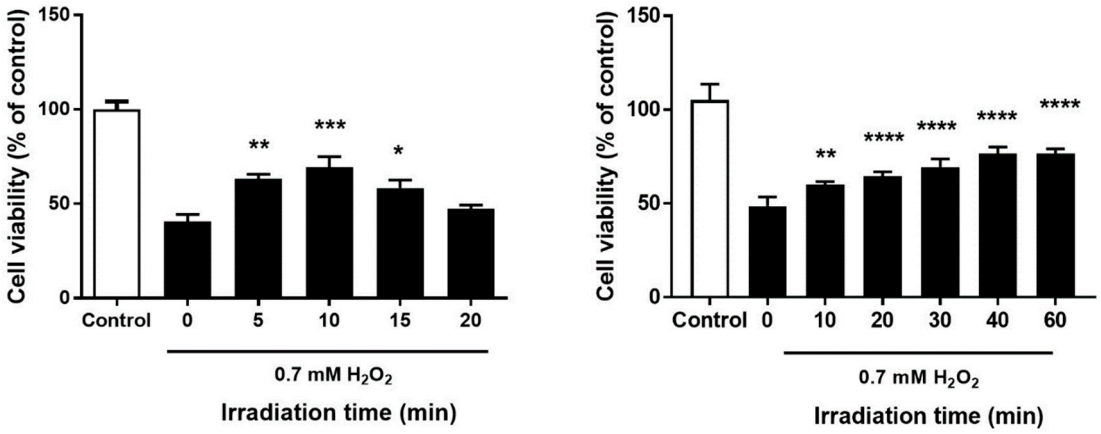


**Figure 3.** Effects of 630 nm and 850 nm LEDs on the cell viability of $H_2O_2$-treated RAW264.7 cells. Cell viability was analyzed by varying the duration of irradiation with 630 nm and 850 nm LEDs after RAW264.7 cells had been treated with 0.7 mM $H_2O_2$. (A) RAW264.7 cells were irradiated using a 630 nm LED with an intensity of 10 mW/cm$^2$ at 5 min intervals for up to 20 min (total energy density: 3, 6, 9, and 12 J/cm$^2$), then cultured to determine cell viability. (B) RAW264.7 cells were irradiated using an 850 nm LED with an intensity of 10 mW/cm$^2$ at 10 min intervals for up to 40 min (total energy density: 6, 12, 18, and 24 J/cm$^2$), then cultured for 48 h to determine cell viability. Cell viability was measured using colorimetric MTT metabolic activity assays. Each experiment was performed ≥ 3 times (n = 3). Data are shown as means ± SDs. *$p < 0.05$, **$p < 0.01$, ***$p < 0.01$, and ****$p < 0.0001$ vs. untreated cells. One-way ANOVA and Tukey's post hoc analyses were performed to compare all experimental conditions.

### *3.4. Inhibition of ROS generation by 630 nm or 850 nm LED irradiation*

To determine whether the antioxidant effects of 630 nm or 850 nm LED irradiation could inhibit cell death, the inhibition of $H_2O_2$-induced ROS generation was assessed with DCFDA staining. As shown in Figure 4A, ROS were generated in non-irradiated cells upon treatment with $H_2O_2$. However,

Preprints (www.preprints.org) | NOT PEER-REVIEWED | Posted: 5 July 2023 doi:10.20944/preprints202307.0212.v1



when RAW264.7 cells were treated with $H_2O_2$ and then irradiated with the 630 nm or 850 nm LED, ROS generation was significantly reduced. Quantification of ROS intensity in each group (using ImageJ software) revealed approximately 7.4- and 12.3-fold reductions of intensity in cells irradiated with the 630 nm and 850 nm LEDs, respectively, after treatment with $H_2O_2$ ($p > 0.01$ and $p > 0.0001$; Figure 4B). Therefore, it was assumed that the inhibition of apoptosis observed after irradiation with 630 nm or 850 nm LED was not only due to inhibition of ROS generation but also by promotion of displacement of free radicals and reduction of oxidative stress load. There was no significant difference in ROS scavenging activity between the two LEDs.

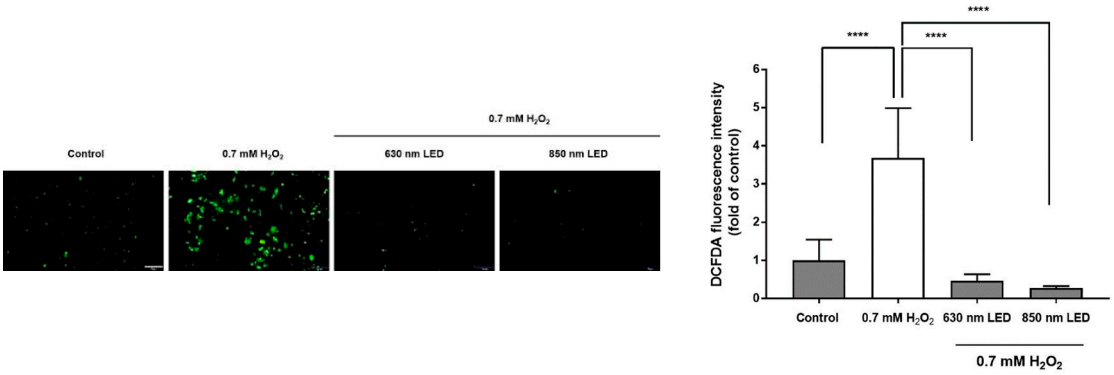


(**A**) (**B**)

**Figure 4.** Radical scavenging activity after 630 nm or 850 nm LED irradiation of $H_2O_2$-treated RAW264.7 cells. (A) Fluorescence image of RAW264.7 cells stained with DCFDA. Cells were observed by fluorescence microscopy (magnification, 400×). Images are representative of three independent experiments (n = 12). Scale bar, 100 $\mu$m. (B) Histogram of the radical scavenging effects of 630 nm or 850 nm LED irradiation in $H_2O_2$-treated RAW264.7 cells. Data are shown as means ± SDs (n = 12). ****$p < 0.0001$ vs. 0.7 mM $H_2O_2$-treated cells. One-way ANOVA and Dunnett's post hoc analyses were performed to compare all experimental conditions.

*3.5. Inhibition of apoptosis after irradiation with the 630 nm or 850 nm LED, as determined by TUNEL staining and flow cytometry*

To investigate whether irradiation with both LED could inhibit apoptosis, $H_2O_2$-treated cells were irradiated with the 630 or 850 nm LED, cultured for 24 h, stained with TUNEL, and observed by fluorescence microscopy to quantify TUNEL-positive cells/nuclei. Among cells that were not treated with $H_2O_2$, few exhibited green fluorescence; after treatment with 0.7 mM $H_2O_2$, most cells exhibited green fluorescence (Figure 5A). However, when $H_2O_2$-treated cells were irradiated with the 630 nm or 850 nm LED, the numbers of TUNEL-positive cells were significantly reduced by approximately 45.7% and 37.8%, respectively, compared with the number among cells that had been treated with 0.7 mM $H_2O_2$ alone ($p < 0.01$ and $p < 0.001$; Figure 5B). The statistical significance between the two LEDs through TUNEL staining could not be confirmed.

To further explore the relationship between cell death inhibition and the stage of apoptosis after LED irradiation of $H_2O_2$-treated RAW264.7 cells, cells were dyed with Annexin V-FITC and PI, then measured by flow cytometric analysis. As shown in Figure 5C and D, 26.1% of $H_2O_2$-treated RAW264.7 cells entered late apoptosis. Among $H_2O_2$-treated cells that were irradiated with the 630 nm or 850 nm LED, the numbers of cells in late apoptosis were approximately 2.3- and 1.8-fold lower, respectively, compared with the number among cells that had been treated with $H_2O_2$ alone. The detailed FACS results are summarized in Table 2. Although it is regrettable that RAW264.7 cells without any treatment have already progressed to the early stage of apoptosis during the incubation process, $H_2O_2$ treatment caused RAW264.7 cells to rapidly enter the late stage of apoptosis, and LED irradiation inhibited this cell death progression. FACS results also could not confirm the statistical significance between the two LEDs (Figure 5D).

Preprints (www.preprints.org) | NOT PEER-REVIEWED | Posted: 5 July 2023 doi:10.20944/preprints202307.0212.v1



**Table 2.** Flow cytometry results.

| Sample | % viable | % apoptotic early | % apoptotic late | % necrotic |
|---|---|---|---|---|
| Control | 25.74 ± 2.70*** | 73.28 ± 2.71 | 0.97± 0.72* | 0 |
| $H_2O_2$ | 9.57 ± 3.79 | 62.80 ± 17.50 | 26.12 ± 11.81 | 1.5 ± 1.34 |
| $H_2O_2$+630 nm | 12.79 ± 0.56 | 75.35 ± 5.67 | 11.53 ± 4.72 | 0.31 ± 0.14 |
| $H_2O_2$+850 nm | 10.69 ± 4.03 | 73.91± 9.83 | 14.78 ± 6.85 | 0.60 ± 0.21 |

Data are the percentage of cells positively stained for Annexin $V^-/PI^-$ (viable cells), Annexin $V^+/PI^-$ (early apoptotic cells), Annexin $V^-/PI^+$ (necrotic cells), and Annexin $V^+/PI^+$ (late apoptotic cells). The experiment was repeated three times (n=3). Data are expressed as the mean ± SD. ****$p < 0.0001$ and *$p < 0.05$ vs. 0.7 mM $H_2O_2$-treated cells.

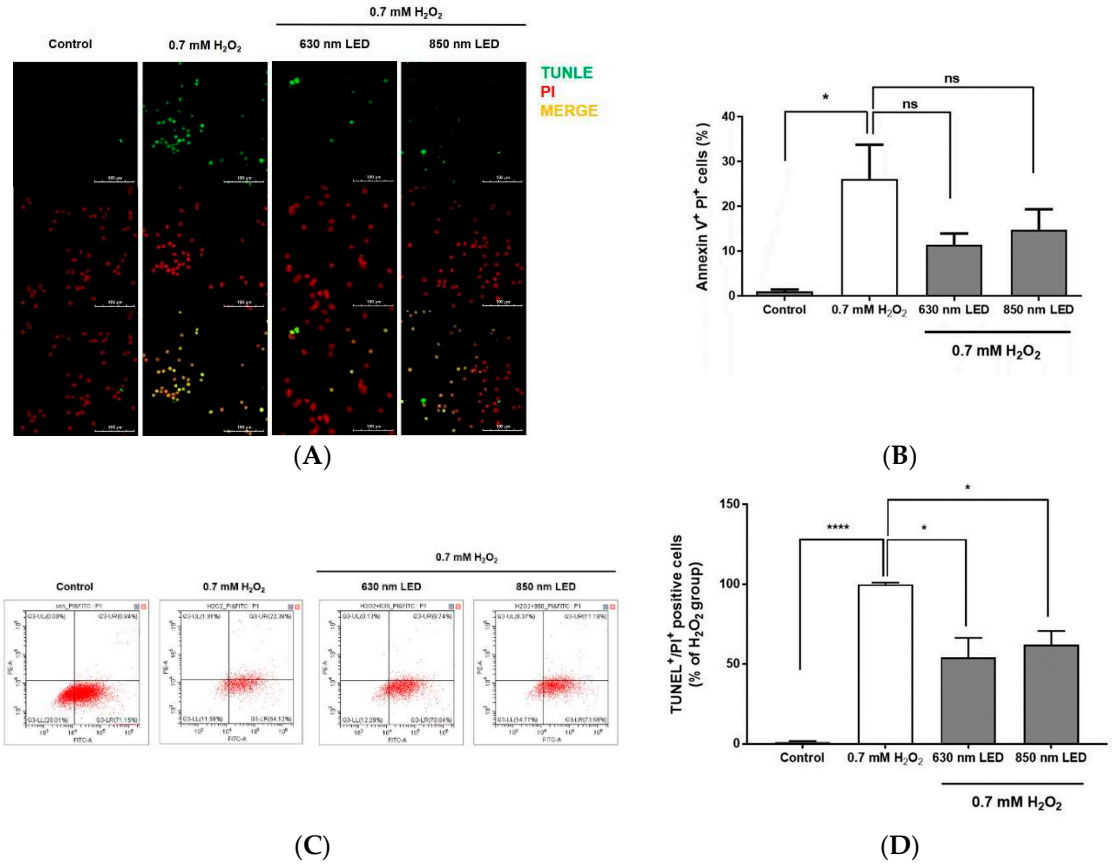


**Figure 5.** Effects of 630 nm or 850 nm LED irradiation on $H_2O_2$-induced apoptosis in RAW264.7 cells, as determined by TUNEL staining and flow cytometry. (A) Representative images of RAW264.7 cells doubly stained with TUNEL (top column) and PI (middle column) under different wavelength conditions (control, 630 nm LED, and 850 nm LED). Cells were observed by confocal microscopy (magnification, 400×). Images are representative of three independent experiments (n = 12). Scale bar, 100 $\mu$m. (B) Bar graph showing the percentage of TUNEL-positive cells relative to PI-positive cells after irradiation with each wavelength. (C) RAW264.7 cells were labeled with Annexin V-FITC and PI, then analyzed by flow cytometry. RAW264.7 cells were cultured for 24 h, treated with $H_2O_2$, then irradiated with 630 nm or 850 nm LED. Dot plots depict cell populations in quadrants. (D) $H_2O_2$-treated RAW264.7 cells were irradiated with 630 nm or 850 nm LED, labeled with Annexin V-FITC and PI, and analyzed by flow cytometry. Histogram shows the percentage of RAW264.7 cells in late apoptosis. Data are shown as means ± SDs (n = 12). ****$p < 0.0001$ and *$p < 0.05$ vs. 0.7 mM $H_2O_2$-treated cells. One-way ANOVA and Dunnett's post hoc analyses were performed to compare all experimental conditions.

### *3.6. Western blotting analysis of the apoptosis-inhibiting effects of the 630 nm and 850 nm LEDs*

The expression level of apoptosis-related proteins was assessed to determine whether the ability to inhibit ROS generation by LED irradiation inhibits apoptosis. After 630 nm LED irradiation of

Preprints (www.preprints.org) | NOT PEER-REVIEWED | Posted: 5 July 2023 doi:10.20944/preprints202307.0212.v1



$H_2O_2$-treated cells, the expression level of Bax was reduced by a smaller amount compared with the expression in cells treated with $H_2O_2$ alone, although this difference was not statistically significant. Although the expression level of Bcl-2 also tended to increase slightly compared with the expression in cells treated with $H_2O_2$ alone, this difference also was not statistically significant. After 850 nm LED irradiation of $H_2O_2$-treated cells, the expression level of Bax was significantly decreased by approximately 1.4-fold compared with the expression in cells treated with $H_2O_2$ alone ($p < 0.01$; Figure 6A,B). Additionally, the expression level of Bcl-2 was significantly increased by approximately 1.1-fold compared with the expression in cells treated with $H_2O_2$ alone ($p < 0.01$; Figure 6A and B). The Bax/Bcl-2 expression ratio in cells irradiated with the 630 nm or 850 nm LED was significantly reduced by approximately 1.3- and 1.6-fold, respectively, compared with the ratio in cells treated with $H_2O_2$ alone ($p < 0.01$ and $p < 0.0001$), indicating that the expression level of Bcl-2 was increased relative to the expression level of Bax after LED irradiation (Figure 6B).

To explore whether irradiation with each LED source inhibited the degradation of procaspase-3 and the cleavage of PARP, the expression levels of these proteins were assessed. As shown in Figure 6C and D, the respective expression levels of procaspase-3 were significantly 1.3- and 1.2-fold greater in 630 nm and 850 nm LED-irradiated cells than in cells treated with $H_2O_2$ alone ($p < 0.01$ and $p < 0.05$). Furthermore, PARP cleavage in cells irradiated with the 630 nm or 850 nm LED was significantly decreased by 2.6- and 1.6-fold, respectively, compared with the cleavage in cells that had been treated with $H_2O_2$ alone ($p < 0.01$ and $p < 0.05$). Although the expression of cleaved caspase 3 could not be confirmed, these results suggest that the inhibition of procaspase 3 degradation by LED irradiation reduced the activation of caspase 3 and inhibited the cleavage of the PARP protein, thereby proceed normal DNA replication and gene expression in cells, which inhibit apoptosis-related signaling. As a result of western blot analysis, statistical significance between the two LEDs could not be confirmed.

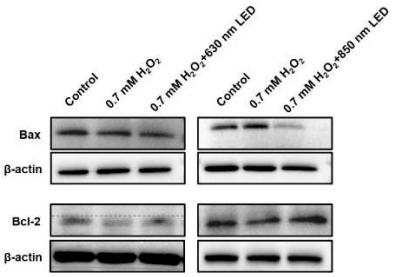


(**A**)

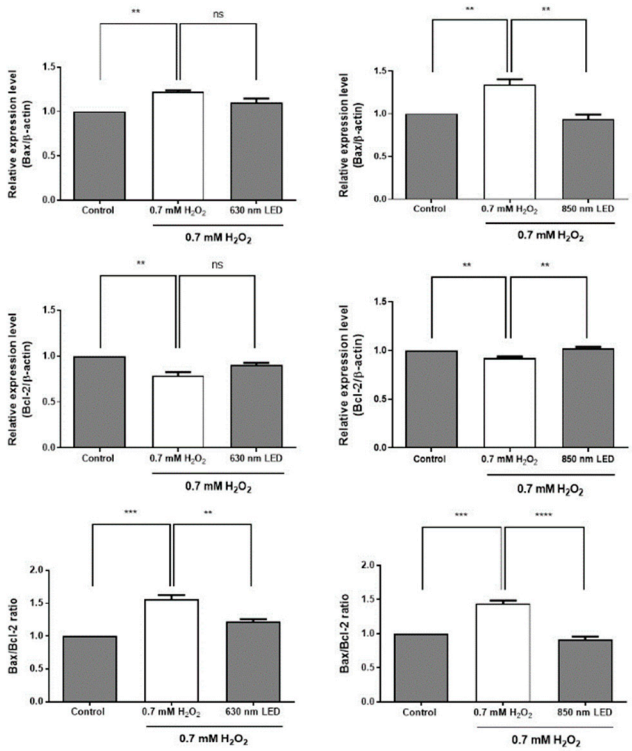


(**B**)

Preprints (www.preprints.org) | NOT PEER-REVIEWED | Posted: 5 July 2023 doi:10.20944/preprints202307.0212.v1



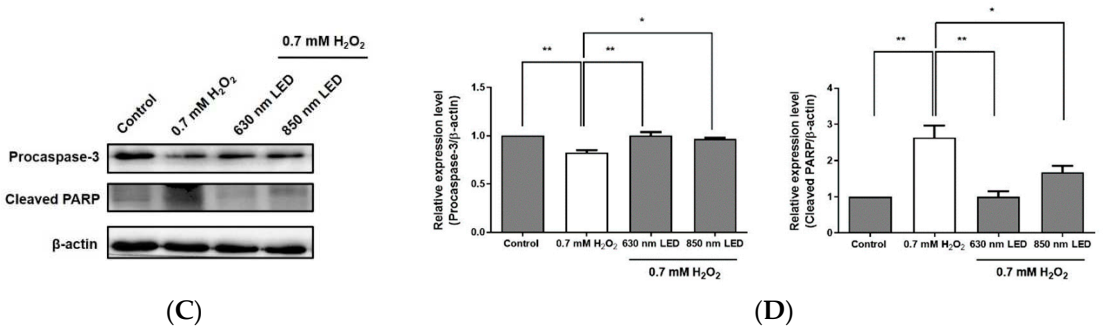


(C) (D)

**Figure 6.** Effects of 630 nm and 850 nm LED irradiation on the Bax/Bcl-2 ratio and the expression levels of procaspase-3 and cleaved PARP in $H_2O_2$-treated RAW264.7 cells. (A) Expression levels of Bcl-2 and Bax were detected using specific antibodies, then quantified using a ChemiDoc Imaging System and the resulting data were used to calculate the Bax/Bcl-2 ratio. (B) $H_2O_2$-treated RAW264.7 cells were irradiated with 630 nm or 850 nm LED, and the expression levels of procaspase-3 and cleaved PARP were analyzed by western blotting. Relative expression levels of procaspase-3 and cleaved PARP-1 are shown in histograms. $\beta$-actin was used as a loading control. Data are shown as means ± SDs. All experiments were performed in triplicate (n = 3). *$p < 0.05$, compared with the control group.

## 4. Discussion

In this study, RAW264.7 cell viability increased over time after 630 nm and 850 nm LED irradiation. Although the mechanism underlying the effects of PBM remains unclear, our results are consistent with former studies that have shown the promotion of cell proliferation, differentiation, and maturation after irradiation with an LED or laser in the wavelength bands of 620 ± 20 nm or 825 ± 25 nm [16, 17]. On the other hand, some conflicting results have also been reported, possibly because different tissues and cells respond with different targets to specific light wavelengths [18, 19]. In figure 3, when $H_2O_2$-treated cells were irradiated with 630 and 850 nm LEDs, the optimal cell viability was shown at 4-fold higher fluence at 850 nm than at 630 nm. These results are explained by the results of George et al, who reported that 825 nm near-infrared irradiation at high fluence produced high production of beneficial ROS and harmful ROS and simultaneously started antioxidant action to produce twice as much ATP as 636 nm to maintain high cell viability [20]. Although many in vitro reports have shown that ROS increase after PBM, we demonstrated that both 630 nm and 850 nm LEDs inhibit $H_2O_2$ oxidative stress-induced ROS generation and rescue RAW264.7 cells from oxidative stress-induced cell death [10, 22–24]. These results are consistent with the findings by Huang et al., who induced oxidative stress in cortical neuron cells using hydrogen peroxide, cobalt chloride, and rotenone; they showed that irradiation with an 810 nm laser could reduce ROS levels in the cultured cortical neurons, preventing cell death [6]. It is also consistent with the findings by Sun et al., who demonstrated anti-inflammatory effects of 625 nm LED irradiation via scavenging of phorbol-12-myristate-13-acetate-induced ROS in HaCaT human keratinocytes [21]. Our results not only show that red and near-infrared LED illumination can help maintain cellular homeostasis, but also provide an accurate explanation of the paradox of the PBM mechanism proposed in many literatures.

It was confirmed through TUNEL staining that 630 nm and 850 nm LED irradiation could inhibit cell death due to oxidative stress in $H_2O_2$-treated RAW264.7 cells. Indeed, when flow cytometry was used to further explore whether 630 nm and 850 nm LED irradiation inhibited oxidative stress-induced cell death, we found significant differences in the numbers of cells in late apoptosis between irradiated and non-irradiated $H_2O_2$-treated cells. Although it was difficult to suppress early apoptosis in the untreated control group in this experiment, the numbers of cells in late apoptosis were significantly reduced after irradiation with 630 nm or 850 nm LEDs, compared with cells that had been treated with $H_2O_2$ alone; these differences suggested a substantial reduction in the overall rate of cell death after irradiation. The two most important groups of proteins in apoptotic signaling are Bcl-2 family proteins and cysteine proteases known as caspases [25]. In many cells and tissues, the

 doi:10.20944/preprints202307.0212.v1



Bax/Bcl-2 ratio may be important in determining susceptibility to apoptosis. When this ratio is low, cells can resist apoptosis. Therefore, the Bax/Bcl-2 ratio can influence the progression of cell death. Previously, Li et al. reported that irradiation with an 810 nm laser led to increases in Bax protein expression and the Bcl-2/Bax ratio in senescent rat skeletal muscle. This irradiation reduced the progression of myocyte apoptosis in sarcopenic muscles [26]. Miracabad et al. used 6-hydroxide dopamine to induce oxidative stress in PC-12 cells; subsequent treatment with curcumin and a 630 nm LED resulted in a decrease in the Bax/Bcl-2 ratio. The reduction in the Bax/Bcl-2 ratio induced by irradiation with a 630 nm LED was able to protect neurons by reducing 6-hydroxide dopamine-induced neuronal cell death [27]. Our results also showed suppression of $H_2O_2$-mediated oxidative stress-induced cell death through reduction of the Bax/Bcl-2 ratio after irradiation with 630 nm and 850 nm LEDs, consistent with previous in vivo findings that PBM-induced suppression of apoptosis was achieved by inhibiting the expression of mitochondrial-derived apoptosis signaling pathway proteins [28–30].

Apoptosis is initiated by an imbalance in the expression levels of Bcl-2 and Bax in a non-normal cellular state, which leads to increased cytochrome C expression and the activation of caspase proteins [31, 32]. In particular, the cleavage of caspase-3 induced by various stimuli is an important priming event for apoptosis. Activated caspase-3 cleaves the DEVD site to activate PARP; this cleavage leads to a reduction in adenosine triphosphate and the initiation of apoptosis [33, 34]. Although the expression of activated caspase-3 could not be confirmed in this study, the expression level of procaspase-3 was not significantly reduced in $H_2O_2$-treated RAW264.7 cells irradiated with the 630 nm or 850 nm LED, compared with cells that had been treated with $H_2O_2$ alone, it was similar to the level in the untreated control group. Notably, PARP cleavage was significantly reduced in $H_2O_2$-treated cells irradiated with the 630 nm or 850 nm LEDs, compared with cells that had been treated with $H_2O_2$ alone. These our results are consistent with the findings by Salehpour et al., who reported that red and near-infrared laser treatment significantly reduced caspase-3 protein levels in an experimental animal model of brain oxidative stress induced by chronic administration of D-galactose [35].

Overall, the expression of Bax and Bcl-2 proteins involved in the mitochondrial apoptosis signaling pathway changed in the direction to inhibit apoptosis through the reduction of ROS level by 630 nm and 850 nm LED irradiation, which ultimately inhibits cell death by reducing procaspase degradation and PARP cleavage. In addition, the 850 nm near-infrared LED showed better results when the irradiation time was longer than that of the 630 nm red LED, but it was found that the cell death inhibitory effect did not change depending on the LED wavelength. These results suggest that it can be a promising candidate for the treatment of chronic human diseases caused by excessive ROS induction. Nevertheless, why the 850 nm near-infrared LED irradiation time should be longer than that of the 630 nm red LED for optimal effect should be further studied and determined in future studies.

## 5. Conclusion

In this study, we showed that 630 nm or 850 nm LED irradiation inhibited $H_2O_2$-induced oxidative stress-induced cell death in RAW264.7 cells. As a result of irradiating LEDs of two wavelengths to cells subjected to oxidative stress by $H_2O_2$, respectively, it was confirmed that the intracellular ROS level was significantly reduced. The ROS scavenging effect by LED irradiation suppressed double-stranded DNA breakage that occurred during apoptosis, and this result led to inhibition of the late apoptosis stage. In addition, the expression of apoptosis pathway proteins in a direction that inhibits apoptosis supported this result.

**Author Contributions:** Conceptualization, J.C.A. and S.J.M.; methodology, H.E.K., E.Y.K. and S.J.M.; investigation, H.E.K. and E.Y.K.; data curation, H.E.K., E.Y.K. and S.J.M.; writing—original draft preparation, H.E.K. and S.J.M.; writing—review and editing S.J.M.; supervision J.C.A. and S.J.M.; project administration, J.C.A. and S.J.M.; funding acquisition, J.C.A. All authors have read and agreed to the published version of the manuscript.

**Funding:** This work was supported by the Korea Foundation for the Advancement of Science & Creativity (KOFAC), and funded by the Korean Government (MOE), supported by Basic Science Research Program through the National Research Foundation of Korea (NRF) funded by the Ministry of Education (NRF-2020R1A6A1A03043283), supported by the National Research Foundation of Korea (NRF) grant funded by the Korea government (Ministry of Science and ICT) (No. 2022R1F1A1062944), supported by Korea Basic Science Institute (National research Facilities and Equipment Center) grant funded by the Ministry of Education (Grant No. 2019R1A6C1010033).

**Institutional Review Board Statement:** Not applicable.

**Informed Consent Statement:** Not applicable.

**Data Availability Statement:** Data are contained within the article.

**Acknowledgments:** Dankook University for administrative and technical support.

**Conflicts of Interest:** The authors declare no conflict of interest.

## References

1. Fiers: W.: Beyaert, R.; Declercq, W.; Vandenabeele, P. More than one way to die: apoptosis, necrosis and reactive oxygen damage. *Oncogene*. **1999**, *18*, 7719-7730.
2. Benzi, G.; Moretti, A. Age- and peroxidative stress-related modifications of the cerebral enzymatic activities linked to mitochondria and the glutathione system. *Free Radic. Biol. Med.* **1995**, *19*, 77-101.
3. Budzynska, B.; Boguszewska-Czubara, A.; Kruk-Slomka, M.; Skalicka-Wozniak, K.; Michalak, A.; Musik, I.; Biala, G. Effects of imperatorin on scopolamine-induced cognitive impairment and oxidative stress in mice. *Psychopharmacology (Berline)*, **2014**, *232*, 931-942.
4. Valko, M.; Leibfritz, D.; Moncol, J.; Cronin, M.T.; Mazur, M.; Telser, J. Free radicals and antioxidants in normal physiological functions and human disease. *Int. J. Biochem. Cell Biol.* **2007**, *39*, 44-84.
5. Byrnes, K.R.; Waynant, R.W.; Ilev, I.K.; Wu, X.; Barna, L.; Smith, K.; Heckert, R.; Gerst, H.; Anders, J.J. Light promotes regeneration and functional recovery and alters the immune response after spinal cord injury. *Lasers Surg. Med.* **2005**, *36*, 171-185.
6. Huang, Y.Y.; Nagata, K.; Tedford, C.E.; McCarthy, T.; Hamblin, M.R. Low-level laser therapy (LLLT) reduces oxidative stress in primary cortical neurons in vitro. *J. Biophotonics.* **2013**, *6*, 829-838.
7. Hamblin, M.R. Shining light on the head: Photobiomodulation for brain disorders. *BBA Clinical*. **2016**, *6*, 113-124.
8. Hamblin, M.R. Mechanisms and Mitochondrial Redox Signaling in Photobiomodulation. *Photochem. Photobiol.* **2018**, 94, 199-212.
9. de Freitas, L.F.; Hamblin, M.R. Proposed mechanisms of photobiomodulation or low-level light therapy. *IEEE J. Sel. Top Quantum. Electron.* **2016**, *22*, 7000417.
10. Chen, A.C.; Arany, P.R.; Huang, Y.Y.; Tomkinson, E.M.; Sharma, S.K.; Kharkwal, G.B.; Saleem, T.; Mooney, D.; Yull, F.E.; Blackwell, T.S.; Hamblin, M.R. Low-level laser therapy activates NF-kB via generation of reactive oxygen species in mouse embryonic fibroblasts. *PLoS One*, **2011**, *6*, e22453.
11. Gao, X.; Xing, D. Molecular mechanisms of cell proliferation induced by low power laser irradiation. *J. Biomed. Sci.* **2009**, *16*, 4.
12. Poyton, R.O.; Ball, K.A. Therapeutic photobiomodulation: nitric oxide and a novel function of mitochondrial cytochrome c oxidase. *Discov. Med.* **2011**, *11*, 154-159.
13. Huang, Y.Y.; Sharma, S.K.; Carroll, J.; Hamblin, M.R. Biphasic dose response in low level light therapy - an update. *Dose Response* **2011**, *9*, 602-618.
14. Mo, S.; Chung, P.S.; Ahn, J.C. 630 nm-OLED accelerates wound healing in mice via regulation of cytokine release and genes expression of growth factors. *Curr. Opt. Photonics* **2019**, *3*, 485-495.
15. Mo, S.; Kim, E.Y.; Ahn, J.C. Effects of 630-nm organic light-emitting diodes on antioxidant regulation and aging-related gene expression compared to light-emitting diodes of the same wavelength. *Curr. Opt. Photonics* **2022**, *6*, 227-235.
16. Huertas, R.M.; Luna-Bertos, E.D.; Ramos-Torrecillas, J.; Leyva, F.M.; Ruiz, C.; García-Martínez, O. Effect and clinical implications of the low-energy diode laser on bone cell proliferation. *Biol. Res. Nurs.* **2014**, *16*, 191-196.
17. Schindl, A.; Merwald, H.; Schindl, L.; Kaun, C.; Wojta, J. Direct stimulatory effect of low-intensity 670 nm laser irradiation on human endothelial cell proliferation. *Br. J. Dermatol.* **2003**, *148*, 334-336.
18. Renno, A.C.; McDonnell, P.A.; Crovace, M.C.; Zanotto, E.D.; Laakso, L. Effect of 830 nm laser phototherapy on osteoblasts grown in vitro on biosilicate® scaffolds. *Photomed. Laser Surg.* **2010**, *28*, 131-133.
19. Chen, Q.; Yang, J.; Yin, H.; Li, Y.; Qiu, H.; Gu, Y.; Yang, H.; Xiaoxi, D.; Xiafei, S.; Che, B.; Li, H. Optimization of photo-biomodulation therapy for wound healing of diabetic foot ulcers in vitro and in vivo. *Biomed. Opt. Express* **2022**, *13*, 2450-2466.

20. George, S.; Hamblin, M.R.; Abrahamse, H. Effect of red light and near infrared laser on the generation of reactive oxygen species in primary dermal fibroblasts. *J. Photochem. Photobiol. B* **2018**, *188*, 60-68.
21. Sun, Q.; Kim, H.E.; Cho, H.; Shi, S.; Kim, B.; Kim, O. Red light-emitting diode irradiation regulates oxidative stress and inflammation through SPHK1/NF-kappaB activation in human keratinocytes. *J. Photochem. Photobiol. B* **2018**, *186*, 31-40.
22. Lubart, R.; Eichler, M.; Lavi, R.; Friedman, H.; Shainberg, A. Low-energy laser irradiation promotes cellular redox activity. *Photomed. Laser Surg.* **2005**, *23*, 3-9.
23. Lavi, R.; Shainberg, A.; Friedmann, H.; Shneyvays, V.; Rickover, O.; Eichler, M.; Kaplan, D.; Lubart, R. Low energy visible light induces reactive oxygen species generation and stimulates an increase of intracellular calcium concentration in cardiac cells. *J. Biol. Chem.* **2003**, *278*, 40917-40922.
24. Zhang, J.; Xing, D.; Gao, X. Low-power laser irradiation activates Src tyrosine kinase through reactive oxygen species-mediated signaling pathway. *J. Cell Physiol.* **2008**, *217*, 518-528.
25. Redza-Dutordoir, M.; Averill-Bates, D.A. Activation of apoptosis signalling pathways by reactive oxygen species. *Biochim. Biophys. Acta* **2016**, *1863*, 2977-2992.
26. Li, F.-H.; Liu, Y.-Y.; Qin, F.; Luo, Q.; Yang, H.-P.; Zhang, Q.-G.; Liu, T.C.-Y. Photobiomodulation on Bax and Bcl-2 proteins and SIRT1/PGC-1$\alpha$ axis mRNA expression levels of aging rat skeletal muscle. *Int. J. Photoenergy* **2014**, *2014*, 1-8.
27. Tabatabaei Mirakabad, F.S.; Khoramgah, M.S.; Tahmasebinia, F.; Darabi, S.; Abdi, S.; Abbaszadeh, H.A.; Khoshsirat, S. The effect of low-level laser therapy and curcumin on the expression of LC3, ATG10 and BAX/BCL2 ratio in PC12 cells induced by 6-hydroxide dopamine. *J. Lasers Med. Sci.* **2020**, *11*, 299-304.
28. Salehpour, F.; Rasta, S.H. The potential of transcranial photobiomodulation therapy for treatment of major depressive disorder. *Rev. Neurosci.* **2017**, *28*, 441-453.
29. da Silva Sergio, L.P.; Thomé, A.M.C.; da Silva Neto Trajano, L.A.; Vicentini, S.C.; Teixeira, A.F.; Mencalha, A.L.; de Paoli, F.; de Souza da Fonseca, A. Low-power laser alters mRNA levels from DNA repair genes in acute lung injury induced by sepsis in wistar rats. *Lasers Med. Sci.* **2019**, *34*, 157-168.
30. Yip, K.K.; Lo, S.C.; Leung, M.C.; So, K.F.; Tang, C.Y.; Poon, D.M. The effect of low-energy laser irradiation on apoptotic factors following experimentally induced transient cerebral ischemia. *Neuroscience* **2011**, *190*, 301-306.
31. Maldaner, D.R.; Azzolin, V.F.; Barbisan, F.; Mastela, M.H.; Teixeira, C.F.; Dihel, A.; Duarte, T.; Pellenz, N.L.; Lemos, L.F.C.; Negretto, C.M.U.; da Cruz, I.B.M.; Duarte, M.M.M.F. *In vitro* effect of low-level laser therapy on the proliferative, apoptosis modulation, and oxi-inflammatory markers of premature-senescent hydrogen peroxide-induced dermal fibroblasts. *Lasers Med. Sci.* **2019**, *34*, 1333-1343.
32. Communal, C.; Sumandea, M.; de Tombe, P.; Narula, J.; Solaro, R.J.; Hajjar, R.J. Functional consequences of caspase activation in cardiac myocytes. *Proc. Natl. Acad. Sci. U. S. A.* **2002**, *99*, 6252-6256.
33. Kaufmann, S.H.; Desnoyers, S.; Ottaviano, Y.; Davidson, N.E.; Poirier, G.G. Specific proteolytic cleavage of poly (ADP-ribose) polymerase: an early marker of chemotherapy-induced apoptosis. *Cancer Res.* **1993**, *53*, 3976-3985.
34. Boulares, A.H.; Yakovlev, A.G.; Ivanova, V.; Stoica, B.A.; Wang, G.; Iyer, S.; Smulson, M. Role of poly (ADP-ribose) polymerase (PARP) cleavage in apoptosis. Caspase 3-resistant PARP mutant increases rates of apoptosis in transfected cells. *J. Biol. Chem.* **1999**, *274*, 22932-22940.
35. Salehpour, F.; Ahmadian, N.; Rasta, S.H.; Farhoudi, M.; Karimi, P.; Sadigh-Eteghad, S. Transcranial low-level laser therapy improves brain mitochondrial function and cognitive impairment in D-galactose-induced aging mice. *Neurobiol. Aging* **2017**, *58*, 140-150.